

# Franck–Condon Dominated Chemistry. Dissociations of Silicon-Centered Radicals Prepared by Femtosecond Reduction of Their Cations in the Gas Phase<sup>†</sup>

Viet Q. Nguyen,<sup>1</sup> Scott A. Shaffer,<sup>1</sup> František Tureček,<sup>\*,1</sup> and Cornelis E. C. A. Hop<sup>2</sup>

Department of Chemistry, University of Washington, Seattle, Washington 98195-1700, and Department of Chemistry, University of Wisconsin, Madison, Wisconsin 53706

Received: March 6, 1995; In Final Form: June 1, 1995<sup>®</sup>

The dimethylhydroxysilyl radical, (CH<sub>3</sub>)<sub>2</sub>Si•OH, (**1**) is generated in the gas phase by collisional neutralization of its cation **1**<sup>+</sup>. Radical **1** undergoes extensive dissociation by C–Si bond cleavage depending on the internal energy of the precursor ion **1**<sup>+</sup>. A small fraction of stable **1** is obtained from vibrationally excited **1**<sup>+</sup>. Significant fractions of stable deuterio analogues of **1**, (CD<sub>3</sub>)<sub>2</sub>Si•OH and (CH<sub>3</sub>)<sub>2</sub>Si•OD, are formed from their corresponding gas-phase cations. Stable CH<sub>3</sub>SiOH molecules and H<sub>2</sub>Si•OH, [CH<sub>3</sub>,SiO]<sup>•</sup>, and (CH<sub>3</sub>)<sub>3</sub>Si• radicals are also formed by collisional neutralization of their cations. Collisional reionization of gas-phase 2-silapropan-2-one results in extensive dissociation of its cation radical. MP4(SDTQ)/6-31+G(d) calculations predict large Franck–Condon effects in the vertical reduction of **1**<sup>+</sup> that deposits up to 229 kJ mol<sup>-1</sup> in the radical formed. Isodesmic and charge-transfer reactions are used to estimate the heat of formation of **1** as -254 kJ mol<sup>-1</sup>, and its adiabatic ionization energy as 6.25 eV. The dissociation energies of the O–H and C–Si bonds in **1** are calculated as 166 and 195 kJ mol<sup>-1</sup>, respectively.

## Introduction

Silicon-centered radicals represent important intermediates in chemical processes ranging from organic synthesis<sup>3</sup> to microprocessor manufacturing.<sup>4</sup> Silicon radicals derived from silanes, alkylsilanes, and silicon halogenides have been studied by a variety of experimental methods in both solution and the gas phase<sup>3,5</sup> and also by theoretical calculations.<sup>6</sup> By contrast, much less is known about oxygenated silicon radicals derived from silyl ethers, R<sub>3</sub>Si–O–, or siloxanes, –O–SiR<sub>2</sub>–O–, which are the building blocks of silicon elastomers and may play a role in elastomer thermal decomposition.<sup>7</sup> Recently, ab initio calculations up to the G2 level of theory<sup>8</sup> have been reported by three groups<sup>9</sup> for simple silicon radicals and molecules of the H<sub>n</sub>SiO<sub>m</sub> type, relevant to the chemistry of silane–oxygen flames.<sup>10</sup>

In this paper we report on the preparation and mass spectral characterization of the dimethylhydroxysilyl radical, (CH<sub>3</sub>)<sub>2</sub>Si•OH (**1**), and some of its major dissociation products. Radical **1** may be viewed as a product of hydroxyl radical addition to dimethylsilylene<sup>11</sup> or hydrogen atom addition to 2-silapropan-2-one,<sup>11,12</sup> both species of significant theoretical<sup>6b</sup> and synthetic interest.<sup>3d</sup> Radical **1** is structurally related to the (CH<sub>3</sub>)<sub>2</sub>SiOH<sup>+</sup> cation, **1**<sup>+</sup>, which is a common fragment observed in the mass spectra of a variety of trimethylsilyl ethers.<sup>13</sup> While readily available in the gas phase, cation **1**<sup>+</sup> has not yet been prepared in the condensed phase.<sup>14</sup> Gas-phase cation **1**<sup>+</sup> provides a convenient precursor for the preparation of its reduced form **1** by fast collisional electron transfer, as implemented in neutralization–reionization mass spectrometry (NRMS).<sup>15</sup> In this method, mass-selected ions of kiloelectronvolt kinetic energy are allowed to collide with thermal atomic or molecular targets. Fast neutrals formed by charge exchange are separated from the residual ions by deflecting or reflecting the latter electrostatically and allowed to drift to another cell where the nondissociating (survivor) molecules and the products of their dissociations are reionized by a second collision, and the

resulting ions are analyzed by mass and detected. The NRMS methodology has been used recently by Schwarz and co-workers<sup>16a–h</sup> and by Gu and Tureček<sup>16i</sup> to successfully generate and characterize several small silicon-containing molecules.<sup>16j</sup>

A characteristic feature of collisional electron transfer at kiloelectronvolt kinetic energies is the very short time of the donor–acceptor interaction (<10<sup>-14</sup> s), resulting in an essentially vertical transition between the ion and neutral potential energy surfaces.<sup>15d</sup> The vertical transition may result in vibrational excitation in the incipient neutral species if its equilibrium geometry and that of its ion precursor differ (Franck–Condon effects). Franck–Condon effects have been shown qualitatively to account for the extensive dissociation of weakly bound species, e.g., CH<sub>3</sub>CO•.<sup>17</sup> In the present work we show that the chemistry of gas-phase silicon-centered radicals is greatly affected by Franck–Condon effects in the reduction step, in keeping with the behavior of other second-row radicals studied by NRMS.<sup>18</sup>

Since reference thermochemical data for oxygenated silicon radicals are scarce,<sup>19</sup> we also report ab initio calculations providing relative enthalpies of the neutral and ionic species in their relaxed geometries and following vertical electron transfer.

## Experimental Part

**Materials.** Trimethylsilylethyl ether and trimethylsilylethyl-d<sub>5</sub> ether were prepared by silylation with hexamethyldisilazane of anhydrous ethanol or ethanol-d<sub>6</sub>, respectively, according to a literature procedure.<sup>20</sup> The products were purified by distillation, bp 75 °C (lit.<sup>20</sup> gives bp 74.5 °C). The 70-eV electron impact mass spectra<sup>21c</sup> of the products showed no volatile impurities. Mass spectrum of (CH<sub>3</sub>)<sub>3</sub>SiOC<sub>2</sub>D<sub>5</sub> (*m/z*, rel intensity): 123 (M<sup>++</sup>, 2), 121(1), 110(4), 109(10), 108 ((M – CH<sub>3</sub>)<sup>+</sup>, 100), 107(2), 78(1), 77(3), 76((CH<sub>3</sub>)<sub>2</sub>SiOD<sup>+</sup>, 42), 75(1), 74(1), 73 ((CH<sub>3</sub>)<sub>3</sub>Si<sup>+</sup>, 7), 62(3), 61(1), 60 (CH<sub>2</sub>SiOD<sup>+</sup>, 12), 59(2), 58(1), 50(1), 48(2), 46(5), 45(3), 44(1), 43(3), 34(4), 33(1), 30(2). (Trimethylsilyl)benzyl ether was prepared by silylation of benzyl alcohol with equivalents of trimethylchlorosilane and pyridine. The product was purified by distillation and its mass spectrum was consistent with the literature data.<sup>13</sup> Tris(methyl-

<sup>†</sup> Dedicated to Dr. Zdenek Herman as a tribute to his contributions to the field of gas-phase ion chemistry.

<sup>®</sup> Abstract published in *Advance ACS Abstracts*, October 1, 1995.

$d_3$ )silyl ethyl ether was prepared by silylation of ethanol with tris(methyl- $d_3$ )chlorosilane (CDN Isotopes, 99% D). 1,1,3,4-Tetramethyl-1-sila-2,5-dioxolane (**2**) and 1,1,3,3,5,6-hexamethyl-1,3-disila-2,4,7-trioxepane (**3**) were prepared in a mixture by treating *rac*-2,3-butanediol with dichlorodimethylsilane and pyridine at room temperature according to a standard procedure.<sup>22</sup> The siloxanes were separated from the polymeric material by short-path distillation and characterized by gas chromatography–mass spectrometry. Mass spectrum of **2** ( $m/z$ , rel intensity): 146 ( $M^{+}$ , 4), 133(9), 132(24), 131(100), 130(4), 129(6), 115(5), 105(4), 104(9), 103(87), 102(44), 101(31), 89(4), 88(8), 87(88), 78(3), 77(47), 76(5), 75(43), 74(3), 73(7), 72(9), 71(5), 61(27), 60(7), 59(45), 58(27), 55(4), 47(12). Mass spectrum of **3** ( $m/z$ , rel intensity): 207(3), 206(6), 205 ( $M - CH_3$ , 33), 187(6), 179(3), 178(6), 177(34), 176(8), 161(3), 151(20), 149(8), 135(12), 134(14), 133(100), 132(3), 119(6), 117(6), 115(5), 105(4), 103(7), 89(4), 88(2), 87(3), 75(8), 74(4), 73(22), 66(6), 61(5), 59(7), 55(19). Trimethylsilanol was prepared from its sodium salt (Aldrich), extracted in ether, and distilled according to literature,<sup>22</sup> bp 100 °C.

**Methods.** Neutralization–reionization ( $^{+}NR^{+}$ ) spectra were obtained on a tandem quadrupole acceleration–deceleration mass spectrometer described previously.<sup>15e,23</sup> Volatile samples were introduced into the ion source from a heated glass inlet system, or from a small glass reservoir maintained at 25 °C; the sample intake was regulated by a needle valve to achieve a  $4 \times 10^{-6}$  Torr pressure in the ion source. Flash-vacuum pyrolysis was carried out in a molecular-flow microoven described previously.<sup>24</sup> Precursor ions were generated by electron impact ionization of the silyl ethers at 70 eV. The precursor ions were passed through a quadrupole mass filter operated in the rf only mode, accelerated to 8200 eV and neutralized by collisions with gaseous  $CH_3SSCH_3$ , NO, cyclopropane, or Xe at pressures such as to achieve 70% transmittance of the precursor ion beam. The remaining ions were separated from the neutral products electrostatically and the latter were reionized by collisions with oxygen at 70% transmittance of the precursor ion beam. The intermediate neutral lifetimes were in the 3.3–4.3  $\mu s$  range for precursor ions of  $m/z$  47–81. Collisionally activated dissociation of the intermediate neutrals ( $^{+}NCR^{+}$ ) was carried out by admitting helium into the differentially pumped neutral drift region<sup>23–25</sup> at a pressure such as to achieve 50% transmittance of the precursor ion beam. The drift region was floated at +250 V, so that any ions formed there by collisional reionization had kiloelectronvolt total energies and were rejected by an energy filter following deceleration.<sup>23</sup> The reported spectra were averaged over 25–40 repetitive scans obtained at scan rates of 1 s (75 data points) per mass unit.

Carrying out mass analysis by linked scanning of the deceleration voltage and the MS-II quadrupole mass filter<sup>23a</sup> but without mass selection of the precursor ion may result in interferences due to two precursor ions at adjacent  $m/z$  forming the same fragment. For example, the fragmentations of precursor ions (or neutrals) of 8200 eV kinetic energy,  $m/z$  81  $\rightarrow$   $m/z$  46, and  $m/z$  82  $\rightarrow$   $m/z$  46 from **1b**<sup>+</sup>, give the products at  $m/z$  46 with 4657 and 4600 eV kinetic energy, respectively, whose peak maxima are resolved by the energy filter.<sup>23</sup> However, if the fragmentations are accompanied by kinetic energy release  $T$ , the kinetic energy width of the  $m/z$  46 peak from  $m/z$  82 is given by<sup>26</sup>

$$\Delta(eU_{dec}) = 4 \times (46/82) \times 8200 [T \times 36/(46 \times 8200)]^{1/2} = 179.75 \sqrt{T}$$

Hence for a nonzero  $T$ , a fraction of  $m/z$  46 ions from the  $m/z$

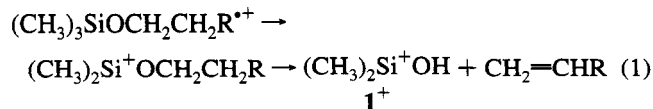
82 precursor will have kinetic energies within the transmission window for  $m/z$  46 from  $m/z$  81 ( $4657 \pm 20$  eV) and appear in the spectrum. For a gaussian distribution of kinetic energy release, a  $T$  in the 50–500 meV (fwhm) range will result in 3–34% of  $m/z$  46 from  $m/z$  82 being cotransmitted with the  $m/z$  46 from  $m/z$  81. For precursor ions differing by  $\geq 2$   $u$  the interferences become negligible even for large  $T$ .

Metastable ion dissociations of mass-selected ions of 8 keV kinetic energy were measured in the second field-free region of a VG ZAB-2F double-focusing mass spectrometer of a reversed (magnet B precedes electrostatic sector E) geometry. Collisionally activated dissociation (CAD) spectra were obtained in a collision cell located in the second field-free region of the VG ZAB-2F instrument. Helium was used as the collision gas at a pressure to achieve 75% transmittance of the precursor ion beam. In these measurements all slits were fully open to obtain maximum signal intensity and to minimize energy resolving effects. The metastable ion and CAD spectra were obtained as single scans. CAD spectra of 4 keV ions were also measured on a Kratos Profile HV-4 instrument equipped with a grounded collision cell mounted in the first field-free region. Oxygen was used as the collision gas at a pressure to allow 70% transmittance of the precursor ion beam. The spectra were obtained by scanning the magnet ( $B$ ) and electrostatic ( $E$ ) sectors while maintaining a constant  $B/E$  ratio ( $B/E$  linked scan).

**Calculations.** Standard ab initio calculations were carried out using the Gaussian 92 set of programs.<sup>27</sup> Spin-unrestricted calculations (UHF) were used for open-shell species. The  $\langle S^2 \rangle$  values in UHF calculations of doublet states were typically in the 0.75–0.77 range, indicating low-spin contamination. Geometries were optimized with the 6-31+G(d) basis sets to obtain local minima that were characterized by harmonic vibrational analysis (all frequencies real). The dissociation of the O–H bond in **1** was investigated with MP2/6-31+G(d) calculations including perturbational Møller–Plesset<sup>28</sup> treatment (frozen core, FC) of electron correlation effects. Zero-point vibrational energies and 298 K enthalpies, the latter calculated within the rigid rotor–harmonic oscillator approximation, were obtained from the harmonic vibrational frequencies calculated with the 6-31+G(d) basis sets and scaled by 0.89.<sup>29</sup> The unscaled harmonic frequencies are given as supporting information. Improved total energies were obtained by single-point calculations on the HF/6-31+G(d) optimized geometries using the Møller–Plesset theory (frozen core) truncated at fourth order with single, double, triple, and quadruple excitations (MP4-(SDTQ)). MP3 total energies were checked and in all cases confirmed convergence of the MP series.

## Results and Discussion

**Ion Dissociations.** Stable  $(CH_3)_2SiOH^{+}$  ions (**1**<sup>+</sup>,  $m/z$  75) were used as precursors for the generation of transient radicals **1**. Ions **1**<sup>+</sup> are formed abundantly by the reaction sequence shown in eq 1, involving methyl loss from an alkyltrimethylsilyl



ether cation radical followed by alkene elimination.<sup>13</sup> In this work we used trimethylsilylethyl ether ( $R = H$ ) whose dissociative ionization gives **1**<sup>+</sup> as the second most abundant ion (85%).<sup>21c</sup> Analogous reaction sequences were used to generate deuterium labeled ions, e.g., dissociative ionization of  $(CH_3)_3SiO-CD_2CD_3$  gave cleanly  $(CH_3)_2Si^{+}OD$  (**1a**<sup>+</sup>), and  $(CD_3)_3SiOC_2H_5$  yielded  $(CD_3)_2Si^{+}OH$  (**1b**<sup>+</sup>). Ions **1**<sup>+</sup> were also

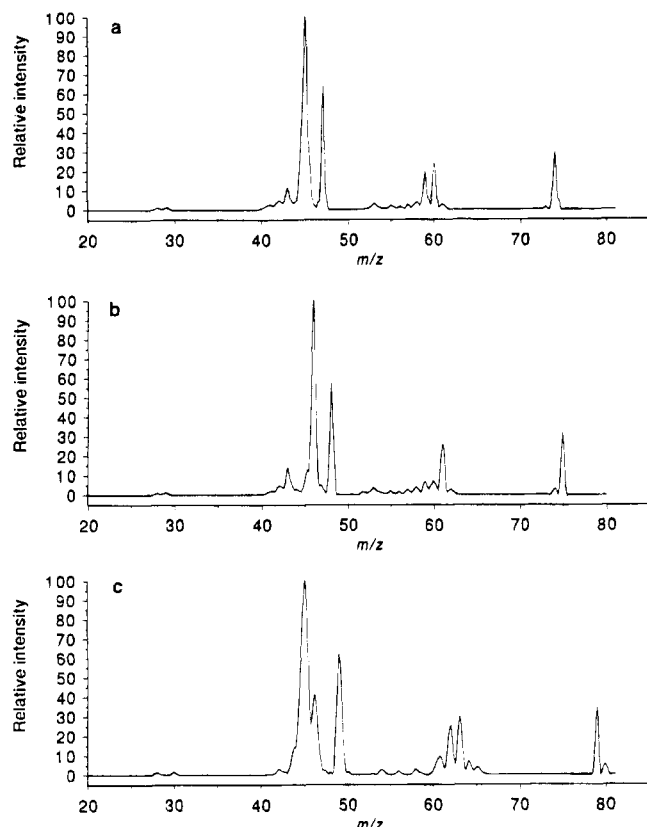
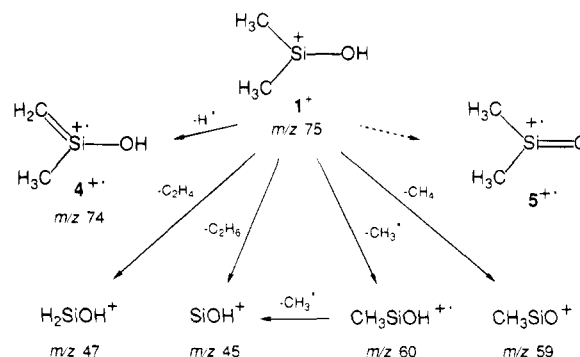


**Figure 1.** Collisionally activated dissociation spectra of (a)  $1^+$ , (b)  $1a^+$ , and (c)  $1b^+$ .

generated by dissociative ionization of trimethylsilanol<sup>21c</sup> and trimethylsilyl 4-hexenyl ether and characterized by their  $^+NR^+$  spectra. Ions  $1^+$  were studied through unimolecular dissociations of metastable ions,<sup>26b,c</sup> and collisionally activated dissociations (CAD) of stable ions.<sup>30</sup> Metastable  $1^+$  of  $\sim 12 \mu s$  lifetime dissociates almost exclusively (95%) by elimination of a molecule of 28 u, which was identified as  $C_2H_4$  by  $^{29}Si$  and  $^2H$  isotope labeling as follows. The isotopomer ions at  $m/z$  76 (6.9% of  $m/z$  75 intensity) consist of 31.9%  $^{13}CCH_7O^{28}Si$  and 68.1%  $^{12}C_2H_7O^{29}Si$  due to the naturally occurring isotopes.<sup>31</sup> Assuming negligible isotope effects on the fragmentation, unimolecular losses from  $m/z$  76 of Si, CO, or  $C_2H_4$  should give  $[m/z 47]/[m/z 48]$  product ion intensity ratios equal to 68.1/31.9, 16/84, and 31.9/68.1 for losses of  $^{28}Si/^{29}Si$ ,  $^{12}CO/^{13}CO$ , and  $^{13}CCH_4/^{12}C_2H_4$ , respectively. The experimental value of 31.8/68.2 points unequivocally to the loss of  $C_2H_4$  from  $1^+$ . In keeping with this finding, metastable  $1b^+$  eliminates cleanly (>95%)  $C_2D_4$  to give  $D_2SiOH^+$  at  $m/z$  49, and metastable  $1a^+$  eliminates  $C_2H_4$  without involvement of the hydroxyl deuterium atom. The mechanism of this hydrogen rearrangement dissociation has not been studied in detail.  $^+NR^+$  mass spectra and ab initio calculations suggest  $H_2SiOH^+$  as a plausible structure for the resulting ion,<sup>16a</sup> as discussed below. By comparison, elimination of ethylene from metastable  $(CH_3)_2C^+-OH$  to give  $CH_2OH^+$ , which is also a major dissociation channel, involves hydrogen exchange between the methyl and hydroxy groups resulting in  $\sim 30\%$  of the OH hydrogen atoms being incorporated in the  $C_2H_4$  molecules eliminated.<sup>32</sup>

Collisional activation of stable  $1^+$  gives rise to several products, as investigated by deuterium labeling. The CAD spectrum of  $1^+$  (Figure 1a) shows a loss of hydrogen radical to give an ion at  $m/z$  74. The CAD spectra of  $1a^+$  (Figure 1b) and  $1b^+$  (Figure 1c) show major peaks due to losses of H and D, respectively, suggesting the formation of the stable 2-silapropen-2-ol cation radical ( $4^{+}$ ) and not its 2-silapropen-2-one

### SCHEME 1



isomer ( $5^{+}$ , Scheme 1). Loss of a methyl forms the methyl-(hydroxy)silylene cation radical at  $m/z$  60, which shows the expected mass shifts on deuterium labeling, e.g.,  $1a^+ \rightarrow m/z$  61 and  $1b^+ \rightarrow m/z$  63 (Figure 1b,c). Elimination of  $CH_4$  gives a  $[C,H_3,O,Si]^+$  ion at  $m/z$  59 ( $m/z$  62 from  $1b^+$ ). Interestingly,  $1a^+$  eliminates both  $CH_3D$  and  $CH_4$ , and the low relative intensity of the  $(M - CH_3D)^+$  ion indicates a primary isotope effect in the transfer of the hydroxyl deuterium atom (Scheme 1). Similar isotope effects have been observed for methane eliminations from deuterium-labeled  $(CH_3)_2SOH^+$ <sup>18a</sup> and  $(CH_3)_2N=CH_2^+$ .<sup>22b</sup> A small fraction of  $1b^+$  eliminates  $CD_4$  ( $m/z$  61), which is consistent with the elimination of  $CH_4$  from  $1a^+$ . By comparison, the  $(CH_3)_2C^+OH$  carba-analogue eliminates methane on CAD, while loss of  $CH_3$  is unimportant.<sup>32</sup> The alternative formation of  $[C,H_3,O,Si]^+$  by sequential losses form  $1^+$  of  $CH_3^+$  and  $H^+$  cannot be a priori excluded; however, the two step process is expected to be much more endothermic than the  $CH_4$  elimination due to the large C–H bond dissociation energy in methane. The dominant CAD product from  $1^+$  is  $SiOH^+$  ( $m/z$  45, Figure 1a), whose formation can be depicted by sequential losses of two methyl groups, or an elimination of ethane. CAD of  $1a^+$  gives mostly  $SiOD^+$  at  $m/z$  46 (Figure 1b), while  $1b^+$  gives  $SiOH^+$  at  $m/z$  45 (Figure 1c). The latter spectrum also shows a peak at  $m/z$  46, which is most likely due to  $CD_3Si^+$ . Note that  $CH_3Si^+$  gives a significant peak at  $m/z$  43 in the CAD spectra of  $1^+$  and  $1a^+$  (Figure 1a,b). The dissociations of  $1^+$  by simple bond cleavages are best compatible with the postulated structure of the dimethyl(hydroxy)silyl cation. Isomeric structures, e.g.,  $CH_2=Si(CH_3)OH_2^+$  or  $CH_3-Si(H)CH_2OH^+$ , would be expected to eliminate water or form  $CH_2OH^+$ , respectively, contrary to the CAD spectral data.

**Neutralization–Reionization.** Neutralization of  $1^+$  was carried out with a series of gaseous targets, Xe, NO, cyclopropane, and  $CH_3SSCH_3$ , of vertical ionization energies decreasing in the 12.13–8.96 eV range.<sup>33</sup> The corresponding  $^+NR^+$  mass spectra obtained following reionization with oxygen were very similar as represented by the spectrum due to neutralization with  $CH_3SSCH_3$  (Figure 2a). The spectrum shows substantial dissociation of  $1$  and/or  $1^+$  upon  $^+NR^+$ . The  $^+NR^+$  survivor ion  $1^+$  is negligibly small for the spectrum of  $1^+$  generated from trimethylsilylethyl ether (0.065%  $\sum I_{NR}$ , Figure 2a) and undetectable for  $1^+$  from trimethylsilyl 4-hexenyl ether. By contrast, the  $^+NR^+$  spectrum of  $1^+$  generated from trimethylsilanol does show a survivor ion of 1.2%  $\sum I_{NR}$  relative abundance (Figure 2b). The survivor ion at  $m/z$  75 from trimethylsilanol is not due to isotopic interferences; the peak of  $(CH_3)_3Si^+$  at  $m/z$  73 is 8% of  $m/z$  75 intensity, contributing only 0.3% of  $(CH_3)_3^{30}Si$  at  $m/z$  75. By comparison, dissociative ionization of  $(CH_3)_3-SiOC_2H_5$  produces  $(CH_3)_3Si^+$  whose peak intensity is 42% of that of the  $m/z$  75 peak, resulting in 1.4% contamination due to the  $^{30}Si$  isotopomer at the latter mass; yet the survivor ion is negligible in the corresponding  $^+NR^+$  spectrum (Figure 2a). The

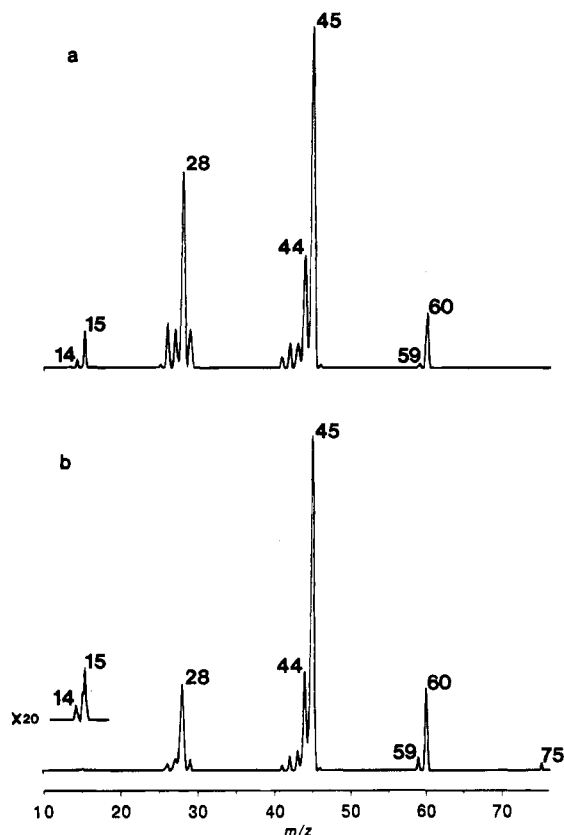


**Figure 2.** Neutralization–reionization ( $\text{CH}_3\text{SSCH}_3$ , 70% $\text{T/O}_2$ , 70% $\text{T}$ ) spectra of  $1^+$  from (a)  $(\text{CH}_3)_3\text{SiOC}_2\text{H}_5$ , (b)  $(\text{CH}_3)_3\text{SiOH}$ .

$(\text{CH}_3)_3\text{Si}^+$  radical is stable when formed by neutralization of its cation (Table 1), as discussed below.

The major  $^+\text{NR}^+$  fragments the spectra of  $1^+$  comprise  $\text{CH}_3\text{-SiOH}^+$  ( $m/z$  60),  $\text{SiOH}^+$  ( $m/z$  45),  $\text{SiO}^+$  ( $m/z$  44),  $\text{Si}^+$ , and  $\text{CH}_3^+$ . The  $^+\text{NR}^+$  spectra of  $1a^+$  and  $1b^+$  both show significant survivor ions (1.3 and 2.4%  $\sum I_{\text{NR}}$ , respectively, Figure 3a,b). However, radical  $1a$  is very sensitive to further excitation as shown by the peak of its survivor ion  $1a^+$ , which decreases to 0.02%  $\sum I_{\text{NR}}$  following neutral collisional activation (Figure 3c). The  $^+\text{NR}^+$  spectra of  $1a^+$  and  $1b^+$  show mass shifts due to deuterium labeling that corroborate the above product assignments. Thus, the hydroxyl deuterium from  $1a^+$  is cleanly retained in  $\text{CH}_3\text{SiOD}^+$  ( $m/z$  61) and  $\text{SiOD}^+$  ( $m/z$  46), which is consistent with the loss of  $\text{CD}_3^+$  ( $m/z$  18) from  $1b$  to form  $\text{CD}_3\text{-SiOH}^+$  ( $m/z$  63) and the formation of  $\text{SiOH}^+$  at  $m/z$  45. It should be noted that the latter spectrum contains interferences from dissociations of  $(\text{CD}_3)_3\text{Si}^+$ , which appear at  $m/z$  50, 48, 46, 44, 42 (corresponding to  $\text{CD}_x\text{Si}^+$ ),  $m/z$  28, 30, 32 (corresponding to  $\text{SiD}_x^+$ ), and in part at  $m/z$  18 and 16 (corresponding to  $\text{CD}_x^+$ ). The nature of these interferences is discussed in the Experimental Part.

An intriguing feature of the  $^+\text{NR}^+$  spectra  $1^+$ ,  $1a^+$ , and  $1b^+$  is the absence of fragments due to losses of  $\text{H}^+$  and  $\text{C}_2\text{H}_4$  (or their isotopomers), whose peaks are quite abundant in the respective CAD spectra (Figure 1a–c). Ion relative abundances in  $^+\text{NR}^+$  spectra are convoluted from contributions of nondissociating ions from reionization of stable neutral fragments, and fragment ions arising by dissociations after reionization. Hence the absence of a particular ion species can be due to several factors, i.e., the absence of a competitive neutral dissociation channel, neutral instability after neutralization, its low reionization efficiency, ion instability after reionization, or absence of a competitive dissociation channel for ion fragment formation.<sup>15d</sup> The latter case may result from a different internal energy distribution in the reionized ion compared to the energy

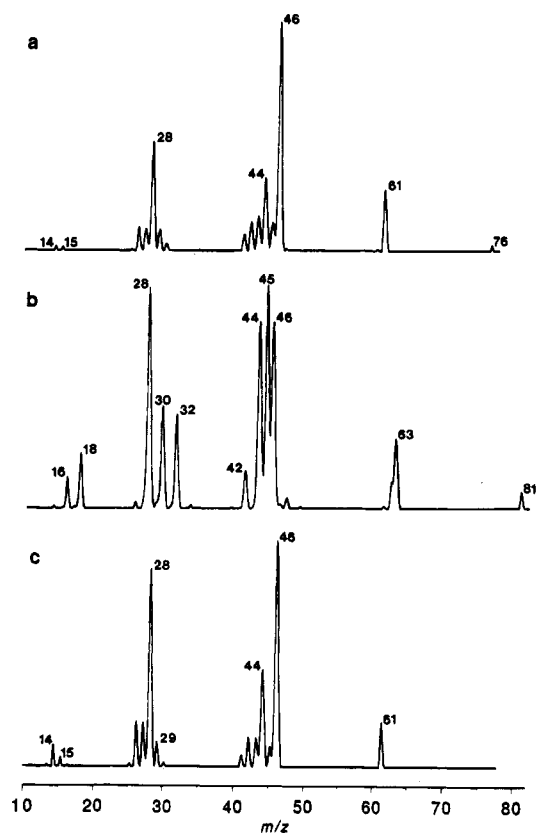


**Figure 3.** Neutralization–reionization spectra of (a)  $1a^+$ , (b)  $1b^+$ , (c)  $^+\text{NCR}^+$  ( $\text{CH}_3\text{SSCH}_3$ , 70% $\text{T/He}$ , 50% $\text{T/O}_2$ , 70% $\text{T}$ ) spectrum of  $1a^+$ .

distribution acquired by ion collisional activation.<sup>24,25,34</sup> To eliminate some of these possibilities, attempts were made at preparation of the missing  $\text{H}_2\text{SiOH}^+$  and  $\text{C}_2\text{H}_6\text{OSi}^+$  ions and examination of their  $^+\text{NR}^+$  spectra.

The  $^+\text{NR}^+$  spectrum of  $\text{H}_2\text{SiOH}^+$ ,  $m/z$  47, generated from trimethylsilylethyl ether, shows an abundant survivor ion (Table 1) proving that the intermediate  $\text{H}_2\text{SiOH}^+$  radical is a stable species under  $^+\text{NR}^+$  conditions, in keeping with the results of Schwarz and co-workers.<sup>16a</sup> The  $^+\text{NR}^+$  spectrum shows sequential losses of up to three hydrogen atoms, with the elimination of  $\text{H}_2$  predominating. The labeled derivative,  $\text{D}_2\text{-SiOH}^+$  from tris(methyl- $d_3$ )silyl ethyl ether, shows a survivor ion and a dominant loss of  $\text{D}_2$  on  $^+\text{NR}^+$  (Table 1). The absence of the peak of  $\text{SiH}^+$  ( $m/z$  29) indicates that there is no  $\text{H/D}$  exchange between the silicon and oxygen bonded hydrogens.<sup>16a</sup> These spectra strongly indicate that the absence of the peak of  $\text{H}_2\text{SiOH}^+$  in the  $^+\text{NR}^+$  spectrum of  $1^+$  is due to an inefficient formation of the radical or the ion by neutral and/or ion dissociations. Note that  $\text{H}_2\text{SiOH}^+$  arises by a complex rearrangement requiring formation and cleavage of several bonds. Such a dissociation is unlikely to be competitive at high internal energies of dissociating ions as documented qualitatively by the decrease of the  $\text{H}_2\text{SiOH}^+$  relative abundance from the metastable ion to the CAD spectrum of  $1^+$ . One may thus conclude that  $1^+$  formed by reionization is highly excited and undergoes preferentially simple bond-cleavage dissociations. This is consistent with previous observations of Hop et al., who reported that relative intensities of fragment ions arising by complex rearrangements were much weaker in the  $^+\text{NR}^+$  spectra than in the metastable ion or CAD spectra.<sup>35</sup>

Loss of  $\text{H}^+$  from  $1$  could give at least two stable neutral products, e.g., 2-silapropen-2-one (**5**)<sup>11b,12</sup> and its less stable<sup>36</sup> enol isomer, 2-silapropen-2-ol (**4**). We sought the cation radicals  $4^{+\bullet}$  and  $5^{+\bullet}$  as precursors for the neutral species, but inspection of the mass spectra database<sup>21c</sup> revealed no obvious

**TABLE 1: Neutralization–Reionization Mass Spectra (CH<sub>3</sub>SSCH<sub>3</sub> (70%T)/O<sub>2</sub> (70%T)) of Silicon Ions**

<i>m/z</i>	relative intensity <sup>a</sup>							
	(CH <sub>3</sub> ) <sub>2</sub> SiOC <sub>2</sub> D <sub>5</sub> <sup>+</sup> <i>m/z</i> 108	(CH <sub>3</sub> ) <sub>2</sub> SiOC <sub>2</sub> H <sub>5</sub> <sup>+</sup> <i>m/z</i> 103	C <sub>2</sub> H <sub>6</sub> OSi <sup>+</sup> <i>m/z</i> 74	(CH <sub>3</sub> ) <sub>3</sub> Si <sup>+</sup> <i>m/z</i> 73	CH <sub>3</sub> SiOH <sup>+</sup> <i>m/z</i> 60	CH <sub>3</sub> SiO <sup>+</sup> <i>m/z</i> 59	D <sub>2</sub> SiOH <sup>-</sup> <i>m/z</i> 49	H <sub>2</sub> SiOH <sup>+</sup> <i>m/z</i> 47
101		0.06						
93	0.03							
91	0.1							
90	0.03							
88		0.1						
87		0.2						
78	0.8							
77	0.2							
75	0.2	0.3						
74	0.3	0.1	0.8					
73		1.1		2.5				
72		0.2						
71		0.06						
63	0.05							
62	0.02							
61	0.3	0.1						
60	0.8	0.06			5.8			
59	1.3	2.2	0.8		1.5	6.3		
58	0.9	1.2	0.3	9.6				
57		0.05						
56	0.6	0.3						
55		0.4						
53	0.3	0.4						
52		0.1						
49						5.5		
48	1.9							
47	0.6	0.2				2.4	11.8	
46	9.8	0.4				5.0	9.0	
45	4.7	7.2	5.0	0.8	59.9	26.3	40.1	
44	14.8	14.8	9.9	4.3	9.4	45.8	16.0	15.5
43	4.9	12.7	9.9	20.2	0.5	15.7		
42	5.8	9.3	6.1	14.9	1.5	8.2		
41	3.5	5.5	3.1	5.6	0.8	0.2		
40	1.5	1.6	0.6					
39		1.3						
38		0.3						
37		0.2						
34	0.5							
33	0.05							
32	10.2							
31	0.6	0.06						
30	12.2	1.0	0.8	0.3		4.6	0.5	
29	2.8	7.9	11.0	8.9	1.8			4.8
28	14.5	13.9	28.0	23.4	16.0	23.8	40.2	17.7
27	10.5	5.5	6.0	4.0				
26	2.2	8.4	9.8	4.6				
25	0.2	1.1	2.5	0.2				
24	0.3	0.2						
18	0.4					(0.2) <sup>b</sup>		
17								0.3
16	0.3	0.05	0.5		0.2	(8.1) <sup>b</sup>		0.3
15	0.04	0.7	2.5	0.7	1.3			
14	0.2	0.3	1.4		0.8	(1.9) <sup>b</sup>		
13	0.4	0.2	0.8		0.5			
12	0.5	0.1	0.2			(1.7) <sup>b</sup>		

<sup>a</sup> Normalized to the sum of reionized ion intensities, % $\Sigma I_{NR}$ . <sup>b</sup> Isobaric interferences from CD<sub>3</sub>SiHD.

sources of C<sub>2</sub>H<sub>6</sub>OSi<sup>+</sup> ions. We found, however, that collisional activation of the C<sub>6</sub>H<sub>5</sub>CH<sub>2</sub>OSi(CH<sub>3</sub>)<sub>2</sub><sup>+</sup> ion results in the formation of C<sub>7</sub>H<sub>7</sub><sup>+</sup> by loss of neutral C<sub>2</sub>H<sub>6</sub>OSi. The latter presumably has the bond connectivity of **5**,<sup>21d-f</sup> and its reionization should give C<sub>2</sub>H<sub>6</sub>OSi<sup>+</sup> at *m/z* 74. Helium CAD of C<sub>6</sub>H<sub>5</sub>CH<sub>2</sub>-OSi(CH<sub>3</sub>)<sub>2</sub><sup>+</sup> followed by collisional ionization of the neutral products showed silicon-containing ions at *m/z* 59, 45 and 28 (Figure 4a). Unfortunately, there is an interference in the spectrum at *m/z* 74 from reionized C<sub>6</sub>H<sub>2</sub><sup>+</sup> that obscures the presence of the isobaric silanone ion. However, the CAD-neutral ionization spectrum of the deuterium-labeled ion, C<sub>6</sub>H<sub>5</sub>-CH<sub>2</sub>-OSi<sup>+</sup>(CD<sub>3</sub>)<sub>2</sub>, is free of interferences at *m/z* 80 (corresponding to C<sub>2</sub>D<sub>6</sub>OSi<sup>+</sup>) and shows a very weak peak corresponding

to ionization of **5-d**<sub>6</sub> (Figure 4b). This indicates that ionization of **5** results in extensive dissociation of the cation radical, making the detection of the molecular ion difficult.<sup>37</sup> For example, the [*m/z* 80]/[*m/z* 62] ratio (0.013 from Figure 4b) and the relative intensity of CH<sub>3</sub>SiO<sup>+</sup> in the <sup>+</sup>NR<sup>+</sup> spectrum of **1**<sup>+</sup> (1.9%  $\Sigma I_{NR}$ , Figure 2b) suggest 0.025% relative intensity for reionized C<sub>2</sub>H<sub>6</sub>OSi<sup>+</sup>, which is at the detection limit of these measurements. These estimates do not include possible differences in internal energies of the intermediate silapropanone molecules originating from (CH<sub>3</sub>)<sub>2</sub>SiOH<sup>+</sup> and C<sub>6</sub>H<sub>5</sub>CH<sub>2</sub>-OSi-(CD<sub>3</sub>)<sub>2</sub><sup>+</sup>, and the deuterium isotope effects in the latter, that will have an effect on the dissociations of the ion after reionization.

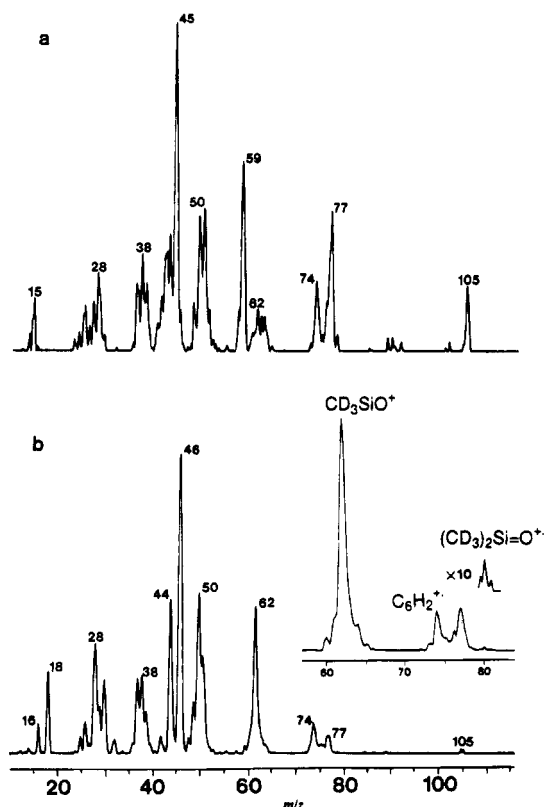
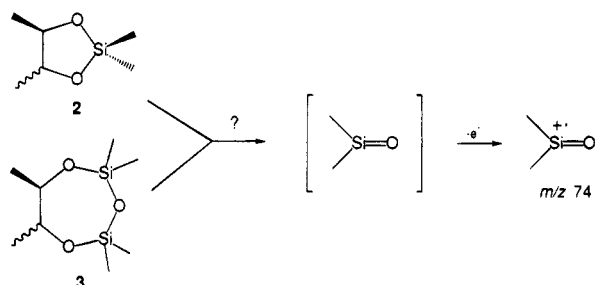


Figure 4. CAD (He, 50%T)/Reionization (O<sub>2</sub>, 70%T) spectra of (a) C<sub>6</sub>H<sub>5</sub>CH<sub>2</sub>OSi(CH<sub>3</sub>)<sub>2</sub><sup>+</sup>, (b) C<sub>6</sub>H<sub>5</sub>CH<sub>2</sub>OSi(CD<sub>3</sub>)<sub>2</sub><sup>+</sup>.

#### SCHEME 2



An attempt at preparation of transient **5** in the ion source was unsuccessful. Flash-vacuum pyrolysis of cyclic siloxanes **2** and **3** (Scheme 2) at 800–1000 °C and  $4 \times 10^{-6}$  Torr yielded a complex mixture<sup>7,12a–c</sup> of products, together with significant fractions of nondecomposed precursors, as documented by the electron-impact mass spectrum.<sup>38</sup> The <sup>+</sup>NR<sup>+</sup> spectrum of the minor C<sub>2</sub>H<sub>6</sub>OSi<sup>+</sup> ion at *m/z* 74 shows a very weak survivor ion (Table 1) whose identity, however, remains ambiguous.

<sup>+</sup>NR<sup>+</sup> spectra were further used to characterize other transient silicon species relevant to the chemistry of **1**. The CH<sub>3</sub>SiOH<sup>+</sup> ion from trimethylsilanol gives a survivor ion in its <sup>+</sup>NR<sup>+</sup> spectrum (Table 1), indicating that the intermediate methylhydroxysilylene, CH<sub>3</sub>SiOH, is a stable species. This is consistent with the stability of the related dimethylsilylene under <sup>+</sup>NR<sup>+</sup> conditions, as reported by Schwarz and co-workers.<sup>16f</sup> The <sup>+</sup>NR<sup>+</sup> spectrum of the [C<sub>2</sub>H<sub>5</sub>SiO]<sup>+</sup> ion generated from trimethylsilanol also shows a survivor ion at *m/z* 59, and a dominant fragment at *m/z* 44 due to loss of CH<sub>3</sub> (Table 1). This and the absence of SiOH<sup>+</sup> and OH<sup>+</sup> in the <sup>+</sup>NR<sup>+</sup> spectrum indicate that the precursor ion contains an intact CH<sub>3</sub> group with the CH<sub>3</sub>–SiO<sup>+</sup> or CH<sub>3</sub>–OSi<sup>+</sup> connectivity. The formation of [C<sub>2</sub>H<sub>5</sub>–Si]<sup>+</sup> (*m/z* 43) and the absence of [C<sub>2</sub>H<sub>5</sub>O]<sup>+</sup> fragments in the NR spectrum point to CH<sub>3</sub>SiO<sup>+</sup>, although an unambiguous proof would require mass spectral analysis of both isomers for

comparison. Note that the stability of a fraction of neutralized [CH<sub>3</sub>O<sub>2</sub>Si]<sup>•</sup> contrasts the facile dissociation upon neutralization of the CH<sub>3</sub>CO<sup>•</sup> carba-analogue.<sup>17</sup> Neutralization of stable H<sub>2</sub>SiOH<sup>+</sup> and SiOH<sup>+</sup> gives rise to stable radicals, H<sub>2</sub>SiOH<sup>•</sup> and SiOH<sup>•</sup>, respectively, that both give abundant survivor ions on reionization (Table 1).<sup>16a</sup> Interestingly, the <sup>+</sup>NR<sup>+</sup> spectrum of the trimethylsilyl ion, (CH<sub>3</sub>)<sub>3</sub>Si<sup>+</sup>, also shows a substantial survivor ion (Table 1), confirming the stability of the intermediate (CH<sub>3</sub>)<sub>3</sub>Si<sup>•</sup> radical formed by vertical neutralization.

**Ab Initio Structures and Relative Energies.** To interpret the CAD and <sup>+</sup>NR<sup>+</sup> spectra and explain the effects due to fast electron transfer, we carried out ab initio calculations of the neutral and ion systems. Experimental thermochemical data are unavailable for most of the species under study.<sup>19</sup> We therefore calculated relative enthalpies of an extensive set of silicon-containing molecules and ions at an intermediate level of ab initio theory, up to MP4(SDTQ)/6-31+G(d) + ZPVE + Δ*H*<sub>298</sub>. The results are summarized in Table 2. The reference value for the Δ*H*<sub>f,298</sub> of radical **1** was anchored through an isodesmic reaction (eq 2) to the standard heats of formation of trimethylsilanol, methylsilane and trimethylsilyl radical, which have been reported with ±6 kJ mol<sup>-1</sup> accuracy.<sup>19,39</sup>

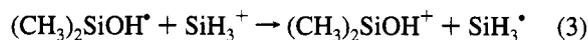


$$\Delta H_{r,0} = 24.7 \text{ kJ mol}^{-1}$$

$$\Delta H_{r,298} = 22.6 \text{ kJ mol}^{-1}$$

$$\Delta H_{f,298}(\mathbf{1}) = -254 \text{ kJ mol}^{-1}$$

The 298 K enthalpies in the ion system were related to the Δ*H*<sub>f,298</sub> of ion **1**<sup>+</sup>, which was anchored through the charge-exchange (isogyric) reaction (eq 3).<sup>39</sup>



$$\Delta H_{r,0} = -170.1 \text{ kJ mol}^{-1}$$

$$\Delta H_{r,298} = -170.0 \text{ kJ mol}^{-1}$$

$$\Delta H_{f,298}(\mathbf{1}^+) = 349 \text{ kJ mol}^{-1}$$

**Ion Thermochemistry.** The calculated dissociation enthalpies in the ion system show that **1**<sup>+</sup> is a stable species whose unimolecular dissociations are substantially endothermic. The lowest thermochemical threshold is calculated for elimination of ethane (Table 3), which, however, may have an activation barrier analogous to those for silicon extrusions from alkylsilanes.<sup>9c,40</sup> An activation barrier is also likely for the elimination of ethene from **1**<sup>+</sup>, which involves two C → Si hydrogen migrations.<sup>6b,41</sup> Although we did not investigate the transition states for these ion rearrangements, the metastable ion and CAD spectra show that elimination of ethene predominates in threshold dissociations and thus is likely to have the lowest energy barrier. Direct bond cleavages in **1**<sup>+</sup> are substantially endothermic; the loss of H is predicted to occur from one of the methyl groups to give the 2-silapropen-2-ol cation radical, which is 97 kJ mol<sup>-1</sup> more stable than the 2-silapropen-2-one ion. This is in complete agreement with the CAD spectra of **1a**<sup>+</sup> and **1b**<sup>+</sup> (vide supra). It is noteworthy that the stabilization of the sila-enol cation radical against the silanone cation radical is much greater than that in the corresponding carba-analogues.<sup>42</sup> Further dissociations of CH<sub>3</sub>–

TABLE 2: Ab Initio Total Energies

species	symmetry electronic state	energy <sup>a</sup>				ZPVE <sup>b</sup>	H <sub>298</sub> <sup>b,c</sup>
		HF	MP2	MP4(SDQ)	MP4(SDTQ)		
(CH <sub>3</sub> ) <sub>2</sub> Si <sup>+</sup> OH	C <sub>1</sub>	-443.396 11	-443.911 33	-443.952 11	-443.965 93	218.6	21.4
(CH <sub>3</sub> ) <sub>2</sub> Si <sup>+</sup> OH (N) <sup>d</sup>	C <sub>1</sub>	-443.346 15	-443.869 97	-443.910 84			
(CH <sub>3</sub> ) <sub>2</sub> SiOH	C <sub>1</sub>	-443.612 45	-444.131 71	-444.174 03	-444.187 57	217.1	21.3
(CH <sub>3</sub> ) <sub>2</sub> SiOH (I) <sup>e</sup>	C <sub>1</sub>	-443.509 46	-444.132 09	-444.084 39	-444.187 80		
CH <sub>2</sub> =Si(OH)CH <sub>3</sub> <sup>+</sup>	C <sub>s</sub>	-442.771 83	-443.258 15	-443.299 12	-443.311 76	187.5	20.4
(CH <sub>3</sub> ) <sub>2</sub> Si=O <sup>+</sup>	<sup>2</sup> A''		-443.259 42		-443.312 48		
(CH <sub>3</sub> ) <sub>2</sub> Si=O <sup>+</sup>	C <sub>s</sub>	-442.744 69	-443.213 33	-443.261 78	-443.274 77	189	20.7
(CH <sub>3</sub> ) <sub>2</sub> Si=O <sup>+</sup> (N) <sup>d</sup>	<sup>2</sup> A''		-443.215 35		-443.276 23		
(CH <sub>3</sub> ) <sub>2</sub> Si=O	C <sub>2</sub>	-442.724 66	-443.190 59	-443.239 63	-443.252 32		
(CH <sub>3</sub> ) <sub>2</sub> Si=O <sup>1</sup> A	C <sub>2</sub>	-443.028 54	-443.564 35	-443.599 93	-443.618 43	191.2	20.1
(E)-CH <sub>3</sub> SiOH <sup>+</sup>	C <sub>s</sub>	-443.714 375	-404.082 64	-404.109 43	-404.119 43	124.0	15.9
(Z)-CH <sub>3</sub> SiOH <sup>+</sup>	<sup>2</sup> A'		-404.084 09		-404.120 26		
(Z)-CH <sub>3</sub> SiOH	C <sub>s</sub>	-403.711 00	-404.077 93	-404.104 57	-404.114 32	122.9	16.2
(Z)-CH <sub>3</sub> SiOH	<sup>2</sup> A'		-404.079 35		-404.115 15		
(E)-CH <sub>3</sub> SiOH	C <sub>s</sub>	-403.977 51	-404.369 48	-404.401 08	-404.411 54	123.8	15.4
(E)-CH <sub>3</sub> SiOH	<sup>1</sup> A'						
CH <sub>3</sub> Si <sup>+</sup> =O	C <sub>3v</sub>	-403.072 01	-403.470 24	-403.489 40	-403.508 66	99.4	14.0
CH <sub>3</sub> Si <sup>+</sup> =O (N) <sup>d</sup>	<sup>1</sup> A <sub>1</sub>						
CH <sub>3</sub> Si=O	C <sub>s</sub>	-403.036 73	-403.448 24	-403.467 35	-403.490 76		
CH <sub>3</sub> Si=O (I) <sup>e</sup>	<sup>2</sup> A'		-403.757 56		-403.795 03	97.1	14.7
CH <sub>3</sub> Si=O	C <sub>3v</sub>	-403.294 28	-403.759 48	-403.779 19	-403.796 17		
CH <sub>3</sub> O=Si <sup>+</sup>	<sup>2</sup> A'		-403.697 33		-403.734 95		
CH <sub>2</sub> SiOH <sup>+</sup>	C <sub>3v</sub>	-403.149 40	-403.703 25	-403.718 13	-403.739 34		
CH <sub>2</sub> SiOH <sup>+</sup>	C <sub>1</sub>	-403.073 70	-403.519 96	-403.548 39	-403.560 45	106.8	13.6
CH <sub>2</sub> SiOH <sup>+</sup>	C <sub>1</sub>	-403.073 70	-403.446 37	-403.475 92	-403.487 02	102.3	12.8
H <sub>2</sub> Si <sup>+</sup> OH	C <sub>s</sub>	-365.260 09	-365.508 67	-365.525 88	-365.531 50	75.5	11.7
H <sub>2</sub> SiOH	<sup>1</sup> A'						
H <sub>2</sub> SiOH	C <sub>1</sub>	-365.513 38	-365.765 77	-365.784 73	-365.790 07	72.2	12.5
H <sub>2</sub> SiOH (I) <sup>e</sup>	C <sub>s</sub>		-365.766 18		-365.790 30		
SiOH <sup>+</sup>	C <sub>s</sub>		-365.651 36		-365.675 96		
SiOH <sup>+</sup>	C <sub>v</sub>	-364.107 89	-364.350 58	-364.366 46	-364.373 13	32.1	10.7
SiOH <sup>+</sup>	<sup>1</sup> Σ		-364.379 02 <sup>f</sup>				
SiOH <sup>+</sup>	C <sub>s</sub>		-364.221 45 <sup>f</sup>				
SiOH	<sup>3</sup> A'						
SiOH	C <sub>s</sub>	-364.338 60	-364.582 50	-364.599 16	-364.605 33	31.1	10.4
SiO	C <sub>s</sub>		-364.584 10		-364.606 30		
SiO	C <sub>v</sub>	-363.784 39	-364.052 67	-364.061 55	-364.075 00	7.4	8.7
SiO <sup>+</sup>	<sup>1</sup> Σ <sub>g</sub>						
SiO <sup>+</sup>	C <sub>v</sub>	-363.399 08	-363.614 43	-363.636 02	-363.644 93	5.8	8.8
SiO <sup>+</sup>	<sup>2</sup> Σ <sub>g</sub>		-363.620 20		-363.649 04		
C <sub>2</sub> H <sub>6</sub>	D <sub>3d</sub>	-79.229 45	-79.497 34	-79.529 00	-79.535 55	186.3	11.8
C <sub>2</sub> H <sub>4</sub>	D <sub>2h</sub>	-78.035 82	-78.290 48	-78.316 20	-78.324 77	128.1	10.5
(CH <sub>3</sub> ) <sub>2</sub> OH <sup>+</sup>	C <sub>s</sub>	-154.384 05	-154.818 68	-154.855 38		233.6	15.6
(CH <sub>3</sub> ) <sub>3</sub> SiOH	<sup>1</sup> A'						
(CH <sub>3</sub> ) <sub>3</sub> SiOH	C <sub>s</sub>	-483.285 37	-483.951 66	-484.008 62	-484.026 31	311.3	26.8
(CH <sub>3</sub> ) <sub>3</sub> SiOH	<sup>1</sup> A''						
CH <sub>3</sub> SiH <sub>3</sub>	C <sub>3v</sub>	-330.273 97	-330.488 85	-330.523 71	-330.528 70	152.5	13.8
SiH <sub>3</sub>	<sup>1</sup> A <sub>1</sub>						
SiH <sub>3</sub>	C <sub>3v</sub>	-290.607 17	-290.676 16	-290.696 48	-290.697 52	53.6	10.4
SiH <sub>3</sub>	<sup>2</sup> A <sub>1</sub>		-290.676 64		-290.697 81		
SiH <sub>3</sub> (I) <sup>e</sup>	D <sub>3h</sub>	-290.594 77	-290.666 39	-290.687 39	-290.688 49		
SiH <sub>3</sub> <sup>+</sup>	D <sub>3h</sub>		-290.668 13		-290.689 55		
SiH <sub>3</sub> <sup>+</sup>	<sup>1</sup> A <sub>1</sub> '	-290.329 32	-290.392 22	-290.410 89	-290.411 64	56.4	10.4
Si	<sup>3</sup> P	-288.832 20	-288.872 86	-288.888 03	-288.888 50		6.2
Si	<sup>3</sup> P		-288.873 51		-288.888 80		
CH <sub>3</sub>	D <sub>3h</sub>	-39.561 10	-39.672 30	-39.691 24	-39.692 96	73.2	11.1
CH <sub>3</sub> <sup>+</sup>	<sup>2</sup> A <sub>2</sub> '		-39.674 15		-39.694 06		
CH <sub>3</sub> <sup>+</sup>	D <sub>3h</sub>	-39.230 89	-39.325 55	-39.345 17	-39.346 29	79.0	10.0
CH <sub>3</sub> <sup>+</sup>	<sup>1</sup> A <sub>1</sub> '						
H <sub>2</sub>	<sup>1</sup> Σ <sup>+</sup>	-1.126 83	-1.144 10	-1.150 81	-1.150 81	24.8	8.7
H	<sup>2</sup> S	-0.498 23					6.2

<sup>a</sup> Hartree; 1 hartree = 2625.5 kJ mol<sup>-1</sup>. For open-shell systems, the lower lines give total energies after spin projection unless stated otherwise (Schlegel, Y. B. *J. Chem. Phys.* **1986**, *84*, 4530). <sup>b</sup> From HF/6-31+G(d) harmonic frequencies scaled by 0.89, kJ mol<sup>-1</sup>. <sup>c</sup> Enthalpy corrections, H<sub>298</sub>-H<sub>0</sub>, calculated from the rigid rotor-harmonic oscillator approximation. <sup>d</sup> Single-point calculations on optimized neutral geometries. <sup>e</sup> Single-point calculations on optimized ion geometries. <sup>f</sup> MP2(FULL)/6-31+G(d) optimizations.

**TABLE 3: MP4(SDTQ)/6-31+G(d) + ZPVE Relative Energies<sup>a</sup>**

reaction	$\Delta H_{f,0}$	$\Delta H_{f,298}$
Ions		
$1^+ \rightarrow \text{CH}_2=\text{Si}(\text{OH})\text{CH}_3^{++} + \text{H}^*$	376	382
$\rightarrow (\text{CH}_3)_2\text{Si}=\text{O}^{++} + \text{H}^*$	473	479
$\rightarrow (E)\text{-CH}_3\text{SiOH}^{++} + \text{CH}_3^*$	392	399
$\rightarrow \text{H}_2\text{SiOH}^+ + \text{C}_2\text{H}_4$	273	274
$\rightarrow \text{SiOH}^+ + \text{C}_2\text{H}_6$	150	151
$\rightarrow (\text{CH}_3)_2\text{OH}^+ + \text{Si}(\text{?P})$	563	563
$(\text{CH}_3)_2\text{Si}=\text{O}^+ \rightarrow \text{CH}_3\text{Si}=\text{O}^+ + \text{CH}_3^*$	177	181
$(\text{CH}_3)_2\text{Si}=\text{O}^+ \rightarrow \text{CH}_3\text{O}=\text{Si}^+ + \text{CH}_3^*$	48	52
$(\text{CH}_3)_2\text{Si}=\text{O}^+ \rightarrow \text{Si}=\text{O}^{++} + \text{C}_2\text{H}_6$	244	244
$(E)\text{-CH}_3\text{SiOH}^+ \rightarrow \text{CH}_3^* + \text{SiOH}^+$	121	127
$(E)\text{-CH}_3\text{SiOH}^+ \rightarrow \text{CH}_3\text{Si}=\text{O}^+ + \text{H}^*$	273	277
$\text{CH}_3\text{Si}=\text{O}^+ \rightarrow \text{CH}_3^+ + \text{SiO}$	216	221
$\rightarrow \text{CH}_3^* + \text{SiO}^{++}$	414	420
$\text{CH}_3\text{O}=\text{Si}^+ \rightarrow \text{CH}_3^+ + \text{SiO}$	345	350
$\text{H}_2\text{SiOH}^+ \rightarrow \text{SiOH}^+ + \text{H}_2$	1	9
Neutral Species		
$1 \rightarrow \text{CH}_3\text{SiOH} + \text{CH}_3^*$	190	195
$\rightarrow (\text{CH}_3)_2\text{Si}=\text{O} + \text{H}^*$	161	166
$\rightarrow \text{CH}_3\text{CH}_3 + \text{SiOH}^*$	121	122
$(E)\text{-CH}_3\text{SiOH} \rightarrow (Z)\text{-CH}_3\text{SiOH}$	6	6
$(E)\text{-CH}_3\text{SiOH} \rightarrow \text{CH}_3^* + \text{SiOH}^*$	278	284
$(E)\text{-CH}_3\text{SiOH} \rightarrow \text{CH}_3\text{SiO}^* + \text{H}^*$	286	292
$(\text{CH}_3)_2\text{Si}=\text{O} \rightarrow \text{CH}_3\text{SiO}^* + \text{CH}_3^*$	316	321
$(\text{CH}_3)_2\text{Si}=\text{O} \rightarrow \text{CH}_3\text{CH}_3 + \text{SiO}$	14	14
$\text{CH}_3\text{SiO}^* \rightarrow \text{CH}_3^* + \text{SiO}$	55	60

<sup>a</sup> In units of  $\text{kJ mol}^{-1}$ .

$\text{SiOH}^{++}$ ,  $(\text{CH}_3)_2\text{Si}=\text{O}^{++}$ , and  $\text{CH}_3\text{Si}=\text{O}^{++}$  are endothermic (Table 3), suggesting that low-energy fractions of these ions should be stable.

The calculations found three equilibrium structures for the  $[\text{C}_2\text{H}_3\text{O}_2\text{Si}]^+$  ions. The most stable one (Table 3) corresponds to the  $\text{CH}_3\text{OSi}^+$  isomer, while  $\text{CH}_3\text{SiO}^+$  and the cyclic  $\text{Si}-\text{CH}_2-\text{OH}^+$  ion are 129 and 187  $\text{kJ mol}^{-1}$  less stable, respectively. No stable linear isomer with the  $\text{CH}_2-\text{Si}-\text{OH}^+$  bond

connectivity has been found. The cyclic  $\text{Si}-\text{CH}_2-\text{OH}^+$  isomer may be viewed as a  $\pi$ -adduct of silicon to  $\text{CH}_2\text{OH}^+$ . The  $[\text{C}_2\text{H}_3\text{O}_2\text{Si}]^+$  isomer relative stabilities differ radically from those of the  $[\text{C}_2\text{H}_3\text{O}]^+$  carba-analogues, for which  $\text{CH}_3\text{CO}^+$  is by far the most stable isomer.<sup>43</sup>

Pertinent to collisional reionization, the calculated total energies of vertically ionized  $1^+$ ,  $(\text{CH}_3)_2\text{Si}=\text{O}^{++}$  ( $5^{++}$ ), and  $\text{CH}_3-\text{Si}=\text{O}^+$  exceed those for the relaxed ions by 108, 59, and 47  $\text{kJ mol}^{-1}$ , respectively, indicating vibrational excitation through Franck–Condon effects. This vibrational excitation alone is insufficient to cause dissociations of the vertically formed  $1^+$  and  $\text{CH}_3\text{Si}=\text{O}^+$  ions, as indicated by the calculated heats of reaction (Table 3). Vertical ionization of relaxed molecule **5** gives ion  $5^{++}$ , which is excited slightly above the dissociation threshold for the formation of  $\text{CH}_3\text{OSi}^+$ , but below that for the formation of  $\text{CH}_3\text{SiO}^+$  (Table 3). Note that the former dissociation must involve a Si  $\rightarrow$  O methyl migration of an unknown activation barrier. We conclude at this point that the extensive decomposition of ionized  $5^{++}$  is likely due to the cumulative effect of the energy content in the neutral precursor, Franck–Condon effects, and collisional activation on ionization. The latter process may deposit up to several electronvolts of internal energy in the ions formed<sup>24,25,34</sup> and promote fast dissociations of weakly bound ions such as  $(\text{CH}_3)_2\text{Si}=\text{O}^{++}$ .

**Neutralization and Neutral Thermochemistry.** The difference between the heats of formation of  $1^+$  and **1** gives an estimate of the adiabatic ionization energy of the radical as  $\text{IE}_a = 6.25 \text{ eV}$ . The  $\text{IE}_a$  value from the MP4+ZPVE energies (from Table 2) is 0.2 eV lower, which difference is typical for calculations with the basis set of a double- $\zeta$  quality.<sup>24b,25</sup> More

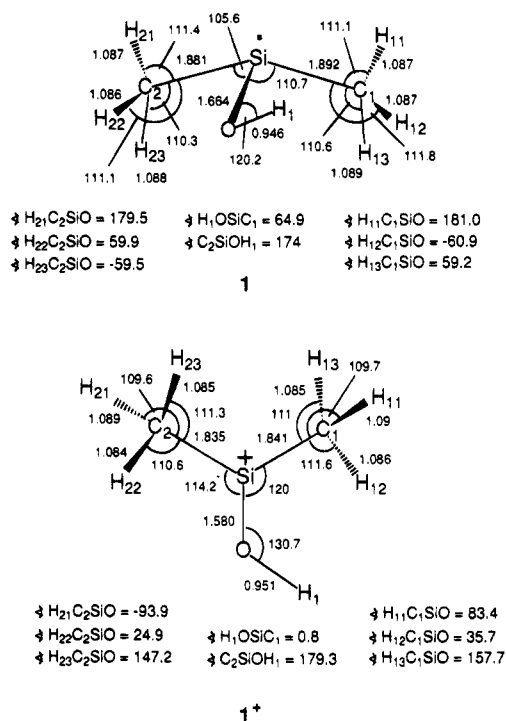


**Figure 5.** HF/6-31+G(d) optimized structures of **1** and **1<sup>+</sup>**. Bond lengths in angstroms, bond angles in degrees.

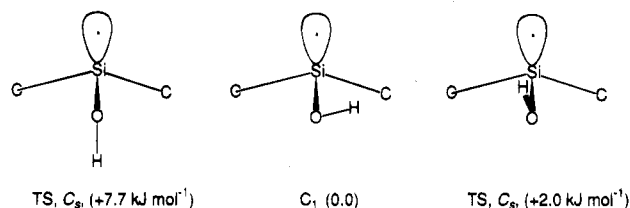


**Figure 6.** Rotation about the Si–O bond in **1**.

importantly, the calculations show large differences between the  $\text{IE}_a$  and the vertical ionization ( $\text{IE}_v$ ) and recombination ( $\text{RE}_v$ ) energies of **1** and **1<sup>+</sup>**, respectively. The MP4(SDTQ) value for  $\text{IE}_a - \text{RE}_v$  (2.37 eV from Table 2) indicates that **1** is formed from relaxed (all  $v = 0$ ) **1<sup>+</sup>** with 229  $\text{kJ mol}^{-1}$  of internal energy as a result of vertical reduction. Likewise, vertical ionization of relaxed **1** requires  $\text{IE}_v = 7.16 \text{ eV}$  (from MP4(SDQ) calculations), suggesting that the ion will be formed with 108  $\text{kJ mol}^{-1}$  of internal energy. The calculations thus indicate very large Franck–Condon effects upon vertical neutralization. The HF/6-31+G(d) optimized structures of **1<sup>+</sup>** and **1** differ substantially (Figure 5). Ion **1<sup>+</sup>** shows a planar  $\text{C}_1\text{C}_2\text{SiOH}$  frame, and a propeller-like conformation of the methyl groups with  $\text{H}_{11}$  and  $\text{H}_{21}$  perpendicular to the C–Si–O plane. Radical **1** is pyramidal at Si and shows longer C–Si and Si–O bonds and smaller C–Si–O angles than does **1<sup>+</sup>** (Figure 5). The  $\text{C}_1$  structure for **1** is the only energy minimum found by the UHF/6-31+G(d) calculations with respect to the rotation about the Si–O bond. Two low-lying  $\text{C}_s$  transition states have been found, one with a syn-periplanar and the other with an antiperiplanar orientation of the O–H bond with respect to the  $z$  axis of the silicon semioccupied  $3p_z$  orbital (Figure 6). A pyramidal  $\text{C}_1$  structure for **1** (available as supporting information) was also obtained from an MP2(FC)/6-31+G(d) optimization. The spin densities from Mulliken population analysis of **1** (Si, 1.2, O, –0.1,  $\text{C}_1$ , –0.05,  $\text{C}_2$ , –0.07) show that the unpaired electron is mostly localized at the silicon atom. The SOMO in **1** is constructed chiefly from the silicon ( $s - p_z + d_{z^2}$ ) atomic orbitals in antibonding combinations with oxygen and carbon ( $-s + p_z$ ) orbitals.

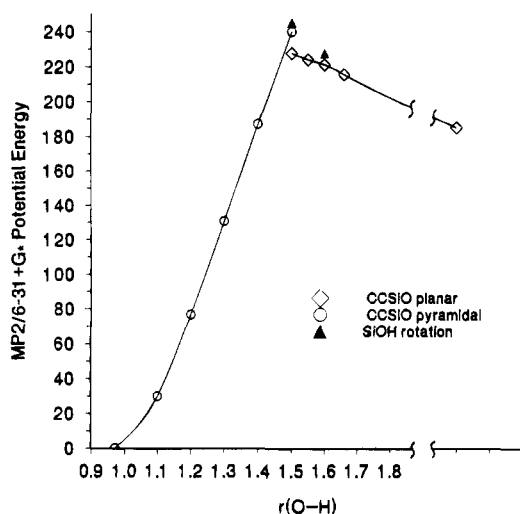


**Figure 7.** MP2(FC)/6-31+G(d) potential energy profile for the O-H bond cleavage in **1**.

Unimolecular dissociations of **1** were investigated for the channels summarized in Table 3. The least endothermic dissociation of **1** is elimination of ethane to give SiOH<sup>•</sup> that requires only 122 kJ mol<sup>-1</sup> at its thermochemical threshold. Simple O-H and Si-C bond cleavages are endothermic by 166 and 195 kJ mol<sup>-1</sup>, respectively. Since the methyl groups are unequal in **1**, Si-C bond dissociation could lead to the syn or anti CH<sub>3</sub>SiOH isomers. The latter is calculated to be only 6 kJ mol<sup>-1</sup> more stable than the former at 298 K. Because of the energy excess in dissociating **1**, both isomers are likely to be formed by the methyl loss. The methyl loss and ethane elimination channels are observed experimentally through the corresponding silicon-containing products, CH<sub>3</sub>SiOH<sup>•+</sup> and SiOH<sup>•+</sup> after reionization, but the hydrogen loss is not. As discussed above the absence of reionized (CH<sub>3</sub>)<sub>2</sub>Si=O<sup>•+</sup> in the NR spectrum of **1**<sup>+</sup> is in part due to facile ion dissociations. To shed some light on the possible formation of (CH<sub>3</sub>)<sub>2</sub>Si=O, we have investigated with MP2(FC)/6-31+G(d) calculations the reaction path for the O-H bond cleavage in **1** as shown in Figure 7. Since stereoelectronic effects are possible due to the mutual orientation of the O-H bond and the semioccupied silicon orbital,<sup>18b</sup> rotation about the Si-O bond was also examined at a few critical points along the O-H coordinate. Stretching of the O-H bond in **1** results in a smooth increase of potential energy; however, the configuration at Si remains pyramidal even for  $r(\text{O-H}) = 1.5 \text{ \AA}$ , and the energy gradient does not indicate surface curvature to a saddle point. Likewise, adding a hydrogen radical to the oxygen atom in 2-silapropan-2-one results in an increasing potential energy, indicating an activation barrier. The configuration at Si remains planar along this part of the reaction path, with the HO-SiC dihedral angle ranging between 75 and 85°. Rotation about the Si-O bond on both branches of the O-H coordinate increases the potential energy by 5–7 kJ mol<sup>-1</sup> (Figure 7) but does not change appreciably the configuration about the silicon atom. Both branches of the reaction path show nonzero gradients in the critical region of  $r(\text{O-H}) = 1.5 \text{ \AA}$  and thus do not converge to a true transition state. We believe that this is an artifact of the MP2 calculations due to an insufficient description of the system by the single-determinant wave function. A multiconfigurational approach would be desirable, which is beyond our capabilities for a system of this size. Nonetheless, the calculations do indicate an activation barrier for the O-H bond cleavage in **1**, which we estimate as 30–40 kJ mol<sup>-1</sup> above the thermochemical threshold for (CH<sub>3</sub>)<sub>2</sub>Si=O + H<sup>•</sup>. An activation barrier for

the cleavage of an O-H bond has been found recently in a related radical system.<sup>18b</sup>

Comparison of the Franck-Condon energy in vertically formed **1** (229 kJ mol<sup>-1</sup>) with the dissociation energies suggests that the radical produced by neutralization of a relaxed (all  $v = 0$ ) **1**<sup>+</sup> should be unstable. However, since ions **1**<sup>+</sup> are formed by dissociative ionization under collision-free conditions, they are likely to have a distribution of vibrational energies ranging from the zero-point energy to the lowest dissociation limit, which is >274 kJ mol<sup>-1</sup> higher (Table 3). The skeletal stretching and deformation vibrations in **1**<sup>+</sup> have low wavenumbers, e.g., (uncorrected) 222 cm<sup>-1</sup> for the symmetrical C-Si-C bend, 259 cm<sup>-1</sup> for the Si out-of-plane skeletal deformation, 649 cm<sup>-1</sup> for the symmetrical O-Si-C<sub>2</sub> stretch, 712 cm<sup>-1</sup> for the H-O-Si in-plane bend, 801 cm<sup>-1</sup> for the asymmetrical C-Si-C stretch combined with CH<sub>3</sub> rock, and 1128 cm<sup>-1</sup> for the O-Si stretch,<sup>44</sup> and thus a substantial fraction of stable **1**<sup>+</sup> are likely to be excited to  $v \geq 1$ . Note that the major differences in the equilibrium geometries of **1** and **1**<sup>+</sup> are in the skeletal bond lengths and angles (Figure 5). Since the collisional electron transfer is faster than the vibrational period,<sup>15d</sup> neutralization of vibrationally excited **1**<sup>+</sup> of nonequilibrium geometry may result in partial relaxation in the radicals formed, resulting in a decrease of the Franck-Condon energy below the 229 kJ mol<sup>-1</sup> level. Hence paradoxically, increasing the fraction of high-energy but stable **1**<sup>+</sup> could increase the fraction of stable **1** formed by vertical neutralization.<sup>45</sup> The spectral data appear to bear out this prediction. Ions **1**<sup>+</sup> prepared by methyl loss from trimethylsilanol are likely to have on average higher internal energies than those prepared by the combined methyl loss and alkene elimination from the trimethylsilyl ethers, because the excess energy in the dissociation is partitioned between the neutral and ion products according to the degrees-of-freedom effect.<sup>46</sup> Consistent with this, neutralization of more energetic **1**<sup>+</sup> from trimethylsilanol results in the formation of a larger fraction of stable **1**, as observed (Figure 2). The deuterium isotope effects on the stability of **1** (Figure 3a,b) can be interpreted as being due to a combination of two factors. The first is the standard kinetic isotope effect due to the zero-point vibrational energies which are estimated to be ~32 and ~151 kJ mol<sup>-1</sup> lower in **1a** and **1b**, respectively, than in **1**.<sup>47</sup> The other is the increased fraction of vibrationally excited **1a**<sup>+</sup> and **1b**<sup>+</sup> due to the lower vibrational frequencies in the deuterated ions, which may increase the fraction of stable **1** formed by vertical reduction.

Neutralization of relaxed H<sub>2</sub>SiOH<sup>•+</sup> is calculated to deposit 299 kJ mol<sup>-1</sup> in the H<sub>2</sub>SiOH<sup>•</sup> radical. The Si-H and O-H bond dissociation energies in H<sub>2</sub>SiOH<sup>•</sup> have been calculated as 224 and 223 kJ mol<sup>-1</sup>, respectively, at the G-2 level of theory.<sup>9b</sup> Although the Si-H bond cleavage may have a ~15 kJ mol<sup>-1</sup> activation barrier,<sup>9c</sup> the vertically formed radical should have sufficient internal energy to dissociate on the  $\mu\text{s}$  time scale. The obvious discrepancy between the prediction on the one hand and the present and previous experiments<sup>16a</sup> on the other is probably due to an overestimation of the Franck-Condon energy by the present calculations. Higher-level calculations using larger basis sets would be necessary to treat this small system adequately.

Neutralization of relaxed CH<sub>3</sub>SiO<sup>•+</sup> is calculated to result in 150 kJ mol<sup>-1</sup> Franck-Condon energy deposited in the CH<sub>3</sub>-SiO<sup>•</sup> radical formed. This exceeds significantly the calculated thermochemical threshold for CH<sub>3</sub>SiO<sup>•</sup> → CH<sub>3</sub><sup>•</sup> + SiO (60 kJ mol<sup>-1</sup>, Table 3). The optimized structures of CH<sub>3</sub>SiO<sup>•+</sup> and CH<sub>3</sub>SiO<sup>•</sup> differ the most in the C-Si and Si-O bond lengths, and in the C-Si-O angle (Figure 8), suggesting that the



- (14) Lambert, J. B.; Schulz, W. J., Jr. In *The Chemistry of Organic Silicon Compounds*; Patai, S., Rapoport, Z., Eds.; Wiley: Chichester, 1989; Vol. 1, Chapter 16, pp 1007–1013.
- (15) (a) Danis, P. O.; Wesdemiotis, C.; McLafferty, F. W. *J. Am. Chem. Soc.* **1983**, *105*, 7454. (b) Burgers, P. C.; Holmes, J. L.; Mommers, A. A.; Terlouw, J. K. *Chem. Phys. Lett.* **1983**, *102*, 1. For recent reviews see: (c) McLafferty, F. W. *Science (Washington, D. C.)* **1990**, *247*, 925. (d) Holmes, J. L. *Mass Spectrom. Rev.* **1989**, *8*, 513. (e) Tureček, F. *Org. Mass Spectrom.* **1992**, *27*, 1087. (f) Terlouw, J. K. *Adv. Mass Spectrom.* **1989**, *11*, 984.
- (16) (a) Srinivas, R.; Bohme, D. K.; Sulzle, D.; Schwarz, H. *J. Phys. Chem.* **1991**, *95*, 9836. (b) Srinivas, R.; Sulzle, D.; Schwarz, H. *J. Am. Chem. Soc.* **1991**, *113*, 52. (c) Srinivas, R.; Sulzle, D.; Koch, W.; DePuy, C. H.; Schwarz, H. *J. Am. Chem. Soc.* **1991**, *113*, 5970. (d) Srinivas, R.; Bohme, D. K.; Hrusak, Schroder, D.; Schwarz, H. *J. Am. Chem. Soc.* **1992**, *114*, 1939. (e) Goldberg, N.; Hrusak, J.; Iraqi, M.; Schwarz, H. *J. Phys. Chem.* **1993**, *97*, 10687. (f) Srinivas, R.; Bohme, D. K.; Schwarz, H. *J. Phys. Chem.* **1993**, *97*, 13643. (g) Iraqi, M.; Goldberg, N.; Schwarz, H. *J. Phys. Chem.* **1993**, *97*, 11371. (h) Iraqi, M.; Schwarz, H. *Chem. Phys. Lett.* **1993**, *205*, 183–186. (i) Gu, F.; Tureček, F. *Org. Mass Spectrom.* **1993**, *28*, 1135. For a recent review see: (j) Zagorevskii, D. V.; Holmes, J. L. *Mass Spectrom. Rev.* **1994**, *13*, 133–154.
- (17) Hop, C. E. C. A.; Holmes, J. L. *Int. J. Mass Spectrom. Ion Processes* **1991**, *104*, 213.
- (18) (a) Gu, M.; Tureček, F. *J. Am. Chem. Soc.* **1992**, *114*, 7146. (b) Tureček, F.; Gu, M.; Hop, C. E. C. A. *J. Phys. Chem.* **1995**, *99*, 2278.
- (19) Walsh, R. In *The Chemistry of Organic Silicon Compounds*; Patai, S., Rapoport, Z., Eds.; Wiley: Chichester, 1989; Vol. 1, Chapter 5, p 374.
- (20) Becke-Goehring, M.; Wunsch, G. *Justus Liebigs Ann. Chem.* **1958**, *618*, 43.
- (21) For leading references to the mass spectra of organosilicon compounds see: (a) Pierce, A. E. *Silylation of Organic Compounds*; Pierce Chemical Co.: Rockford, IL, 1968; Chapter 3, pp 33–39. (b) Schwarz, H. In *The Chemistry of Organic Silicon Compounds*; Patai, S., Rapoport, Z., Eds.; Wiley: Chichester, 1989; Vol. 1, Chapter 7, pp 445–510. (c) McLafferty, F. W.; Stauffer, D. B. *The Wiley/NBS Registry of Mass Spectral Data*; Wiley: New York, 1989; Vol. 1, p 113. (d) Philipou, G. *Org. Mass Spectrom.* **1977**, *12*, 261. (e) Swaim, R. E.; Weber, W. P.; Boettger, H. G.; Evans, M.; Bockhoff, F. M. *Org. Mass Spectrom.* **1980**, *15*, 304. (f) Tsai, R. S.-C.; Larson, G. L.; Oliva, A. *Org. Mass Spectrom.* **1979**, *14*, 364.
- (22) Pawlenko, S. In *Methoden der Organischen Chemie, Band XIII/5: Organo-Silicium Verbindungen*, Muller, E., Bayer, O., Eds.; Thieme: Stuttgart, 1980; pp 138, 191.
- (23) (a) Tureček, F.; Gu, M.; Shaffer, S. A. *J. Am. Soc. Mass Spectrom.* **1992**, *3*, 493. (b) Shaffer, S. A.; Tureček, F.; Cerny, R. L. *J. Am. Chem. Soc.* **1993**, *115*, 12117.
- (24) Kuhns, D. W.; Tran, T. B.; Shafer, S. A.; Tureček, F. *J. Phys. Chem.* **1994**, *98*, 4845.
- (25) Shaffer, S. A.; Tureček, F.; Cerny, R. L. *J. Am. Chem. Soc.* **1993**, *115*, 12117–12124.
- (26) (a) Cooks, R. G.; Beynon, J. H.; Caprioli, R. M.; Lester, G. R. *Metastable Ions*; Elsevier: Amsterdam, 1977. (b) Holmes, J. L.; Terlouw, J. K. *Org. Mass Spectrom.* **1980**, *15*, 383. (c) Holmes, J. L. *Org. Mass Spectrom.* **1985**, *20*, 169.
- (27) Gaussian 92, Revision C; Frisch, M. J.; Trucks, G. W.; Head-Gordon, M.; Gill, P. M. W.; Wong, M. W.; Foresman, J. B.; Johnson, B. G.; Schlegel, H. B.; Robb, M. A.; Replogle, E. S.; Gomperts, R.; Andres, J. L.; Raghavachari, K.; Binkley, J. S.; Gonzalez, C.; Martin, R. L.; Fox, D. J.; DeFrees, D. J.; Baker, J.; Stewart, J. J. P.; Pople, J. A. Gaussian Inc., Pittsburgh, PA, 1992.
- (28) Möller, C.; Plesset, M. S. *Phys. Rev.* **1934**, *46*, 618.
- (29) Curtiss, L. A.; Raghavachari, K.; Pople, J. A. *J. Chem. Phys.* **1993**, *98*, 1293.
- (30) Busch, K. L.; Glish, G. L.; McLuckey, S. A. *Mass Spectrometry/Mass Spectrometry*; VCH Publishers: New York, 1988; pp 107–152.
- (31) McLafferty, F. W.; Tureček, F. *Interpretation of Mass Spectra*, University Science Books: Mill Valley, 1993; Chapter 2, pp 19–34.
- (32) Harrison, A. G.; Gaumann, T.; Stahl, D. *Org. Mass Spectrom.* **1983**, *18*, 517.
- (33) Levin, R. D.; Lias, S. G. *Ionization Potential and Appearance Potential Measurements 1971–1981*, NSRDS-NBS 71, U.S. Government Printing Office, Washington, D.C. 1982.
- (34) (a) Kuhns, D. W.; Tureček, F. *Org. Mass Spectrom.* **1994**, *29*, 463. (b) Beranova, S.; Wesdemiotis, C. *J. Am. Soc. Mass Spectrom.* **1994**, *5*, 1093.
- (35) Hop, C. E. C. A.; van den Berg, K.-J.; Holmes, J. L.; Terlouw, J. K. *J. Am. Chem. Soc.* **1989**, *111*, 72.
- (36) Gordon, M. S.; George, C. *J. Am. Chem. Soc.* **1984**, *106*, 609.
- (37) Maltsev, A. K.; Khabashesku, V. N.; Nefedov, O. N.; Zelinsky, N. D. In ref 3d, Chapter 21, pp 211–224.
- (38) The 70-eV electron-impact mass spectrum of the pyrolysate gives (*m/z*, % base peak): 103(34), 102(15), 101(17), 89(10), 88(16), 87(100), 86(24), 77(79), 75(88), 74(15), 73(92), 72(29), 71(13), 66(35), 61(49), 60(13), 59(70), 58(39), 57(9), 55(46), 45(20), 43(20), 29(12).
- (39) The pertinent heats of formation are as follows: (CH<sub>3</sub>)<sub>3</sub>SiOH (–500 kJ mol<sup>-1</sup>); SiH<sub>3</sub><sup>+</sup> (194 kJ mol<sup>-1</sup>), CH<sub>3</sub>SiH<sub>3</sub> (–29 kJ mol<sup>-1</sup>), SiH<sub>3</sub><sup>+</sup> (967 kJ mol<sup>-1</sup>) (see: Doncaster, A. M.; Walsh, R. *J. Chem. Soc., Faraday Trans. 2* **1986**, *82*, 707). The heat of formation of SiH<sub>3</sub><sup>+</sup> is based on the most recent adiabatic ionization energy of SiH<sub>3</sub><sup>\*</sup> (8.01 eV, Berkowitz, J.; Greene, J. P.; Cho, H.; Ruscic, R. *J. Chem. Phys.* **1987**, *86*, 1235).
- (40) (a) Withnall, R.; Andrews, L. *J. Phys. Chem.* **1985**, *89*, 3261. (b) Gordon, M. S.; Truong, T. N. *Chem. Phys. Lett.* **1987**, *142*, 110. For alkane eliminations from trialkylsilane cation-radicals see: (c) Saulys, D. A.; Hop, C. E. C. A.; Gaines, D. F. *J. Am. Soc. Mass Spectrom.* **1994**, *5*, 537.
- (41) Kudo, T.; Nagase, S. *J. Phys. Chem.* **1984**, *88*, 2833.
- (42) The experimental estimate for Δ*H*<sub>f</sub>(acetone<sup>•+</sup>) – Δ*H*<sub>f</sub>(2-propenol<sup>•+</sup>) is 58 kJ mol<sup>-1</sup> (Lias, S. G.; Bartmess, J. E.; Liebman, J. F.; Holmes, J. L.; Levin, R. D.; Mallard, G. W. *J. Phys. Chem. Ref. Data* **1988**, *17*, Supplement 1, p 119). The most recent G2 ab initio calculations give 39.6 kJ mol<sup>-1</sup> at 298 K (Tureček, F.; Cramer, C. J., unpublished results).
- (43) Nobes, R. H.; Radom, L. *Org. Mass Spectrom.* **1986**, *21*, 407.
- (44) (a) Smith, A. L. *Spectrochim. Acta* **1960**, *16*, 87. (b) Colthup, N. B.; Daly, L. H.; Wiberley, S. E. *Introduction to Infrared and Raman Spectroscopy*, 2nd ed.; Academic Press: New York, 1975; pp 338–342.
- (45) (a) Holmes, J. L.; Sirois, M. *Org. Mass Spectrom.* **1990**, *25*, 481. (b) Sirois, M.; George, M.; Holmes, J. L. *Org. Mass Spectrom.* **1994**, *29*, 11.
- (46) (a) Bente, P. F. III.; McLafferty, F. W.; McAdoo, D. J.; Lifschitz, C. *J. Phys. Chem.* **1975**, *79*, 713 (b) Gilbert, R. G.; Smith, S. C. *Theory of Unimolecular and Recombination Reactions*; Blackwell: Oxford, 1990; p. 70.
- (47) The pertinent O–H and C–H stretching frequencies in **1**, corrected by 0.89, are 3700, 2917, 2904, 2899, 2894, 2841, and 2835 cm<sup>-1</sup>.